CIENTIFIC Publishing Limited

Digital Technologies Research and Applications
http://ojs.ukscip.com/index.php/dtra

Article

Perfect Sequences Based on Golay Codes for Communication Systems

João S. Pereira [1,2,3,*] **and Humberto D. Ferreira** [1,4]

[1] Department of Computer Science, Regional University Network.EU, Polytechnic University of Leiria, School of Technology and Management, Leiria 2400-822, Portugal
[2] Research Centre, "Instituto de Telecomunicações," Leiria 2400-822, Portugal
[3] Research Centre in Informatics and Communications - CIIC, Leiria 2400-822, Portugal
[4] Department of Computer Science, University of Beira Interior, Covilhã 6201-001, Portugal
[*] Correspondence: joao.pereira@ipleiria.pt

Received: 10 January 2024; **Revised:** 30 January 2024; **Accepted:** 26 February 2024; **Published:** 30 March 2024

Abstract: In data transmission systems, ensuring reliable communication while maximizing spectrum efficiency is a challenge. Code Division Multiple Access (CDMA) systems, widely used in wireless networks, depend on spreading codes to manage interference and support users. Achieving a balance between low cross-correlation and optimal autocorrelation properties is complex and involves trade-offs that affect system performance, especially as modern systems demand higher data rates and efficiency. In systems that use spectral spreading, achieving optimal autocorrelation characteristics often compromises cross-correlation characteristics, and vice versa. Codes with low cross-correlation values typically exhibit high out-of-phase autocorrelation values. Therefore, a balance between autocorrelation and cross-correlation properties is necessary for an efficient CDMA communication system. These desirable correlation properties are crucial in both periodic and aperiodic contexts. Recent innovations have led to a patented code generator derived from Golay codes/sequences, which exhibits low periodic cross-correlation values and a periodic autocorrelation function characterized by a prominent correlation peak and null values surrounding it. This development not only enhances signal quality but also mitigates interference in multi-user communication scenarios, making it particularly relevant for modern wireless networks. Furthermore, a novel solution is proposed to minimize the Peak-to-Average Power Ratio (PAPR) and reduce the cost of a new Orthogonal Perfect Discrete Fourier Transform Golay (OPDG) power transmission circuit. This approach leverages advanced signal processing techniques to achieve energy efficiency, addressing a critical challenge in high-performance communication systems. Experimental results demonstrate the practicality of these innovations in real-world implementations, paving the way for future advancements in CDMA technology.

Keywords: Perfect Sequences, OPDG codes, PAPR

1. Introduction

In many communication systems, such as Code Division Multiple Access (CDMA) and Orthogonal Frequency Di-

vision Multiple Access (OFDMA), the need for suitable coding sequences is paramount. These sequences must exhibit excellent periodic autocorrelation and near-perfect cross-correlation features to ensure effective synchronization and code identification in noisy environments. Popular orthogonal codes used in CDMA include Golay sequences [1], Frank and Chu codes [2], and Gold codes [3]. A perfect sequence is a complex sequence where all out-of-phase periodic auto-correlation values are zero. Unfortunately, perfect bipolar sequences longer than 4 and perfect quadri-phase sequences longer than 16 are currently unknown [4].

To achieve higher data rates and improved spectral efficiency, communication systems using OFDMA employ linear modulation techniques like quadrature phase-shift keying and quadrature amplitude modulation [5]. However, a significant challenge is the high Peak-to-Average Power Ratio (PAPR) of the transmitted Orthogonal Frequency Division Multiple (OFDM) signal. High PAPR results in performance degradation due to nonlinear distortion from High-Power Amplifiers (HPAs). This non-linearity leads to in-band distortion, which increases Bit Error Rate (BER), and out-of-band radiation, causing adjacent channel interference [6]. Thus, addressing the PAPR issue is critical for maintaining system power efficiency and minimizing nonlinear distortion in future wireless communication systems [7].

Pereira and Silva [8] introduced a patented Coder/Decoder (CODEC) with perfect sequences of length 2N ($N \in \mathbb{N}$), based on the Inverse Discrete Fourier Transform (IDFT) of Golay sequences [1]. These Golay sequences are not the well-known error correcting code invented by Golay. These new obtained codes are perfect sequences and complementary, unaffected by multipath Interferences (MPI) due to their correlation properties. Termed Orthogonal Perfect DFT Golay (OPDG) codes, or simply Perfect Golay codes, they exhibit satisfactory correlation properties. This paper presents an OPDG code generator to simplify the hardware implementation of lengthy perfect bipolar and quadri-phase sequences. Additionally, a novel solution to reduce PAPR and offer an economical OPDG power transmission circuit is proposed.

Section 2 reviews the concept of Perfect Sequences, while Section 3 introduces the OPDG Codec. Section 4 discusses a solution for the error probability and section 5 shows a PAPR solution based on a binary decomposition of OPDG codes. A conclusion is written at the end.

2. Perfect Sequences

In the study of stochastic processes, particularly those that are Wide-Sense Stationary (WSS), understanding the nature of perfect sequences is crucial. We should remember that, as noted by Theodoridis [9], for any WSS stochastic process, there is a unique autocorrelation sequence that characterizes it. However, the reverse is not true; a single autocorrelation sequence may correspond to multiple WSS processes. Recall that the autocorrelation function correspond to the mean value of the product of random variables, but many different random variables may share the same mean value. The Fourier transform $S_\eta(\omega)$ of an autocorrelation sequence $r(k)$ is nonnegative. Furthermore, if a sequence $r(k)$ has a nonnegative Fourier transform, it is positive definite, and we can always construct a WSS process with $r(k)$ as its autocorrelation sequence. Thus, the necessary and sufficient condition for a sequence to be an autocorrelation sequence remains the nonnegativity of its Fourier transform.

One common example of a WSS process is the white noise [9] sequence. White noise is essential in signal processing and communication systems. It is a random signal characterized by equal intensity at different frequencies, resulting in a constant power spectral density. The mean of white noise is zero, and its autocorrelation function is zero for any non-zero time shifts.

Instead of modeling the input signals using a white noise signal, we will use a discrete u_n sequence generated by a Codec described in the next section. This u_n can be a periodic sequence of length N, where the index point $n = 0,1,2 \ldots, N-1$. Its Discrete Fourier Transform (DFT) [10] is defined by the following expression (1):

$$DFT[u_n] = U_k = \sum_{n=0}^{N-1} u_n W_N^{kn}. \quad (1)$$

The Inverse Discrete Fourier Transform (IDFT) [10] can be expressed as follows (2):

$$IDFT[U_k] = u_n = \frac{1}{N}\sum_{k=0}^{N-1} U_k W_N^{-kn}. \quad (2)$$

For convenience of notation W_N is defined to be (3)

$$W_N = exp(-j\omega) = exp\left(-j\frac{2\pi}{N}\right), \text{ where } j = \sqrt{-1}. \quad (3)$$

Using the DFT and IDFT transformations, periodic cross-correlation can be defined [10, 11] by the following expression (4):

$$r_{uv}[n] = \sum_{k=0}^{N-1} u_k v^*_{mod\,[k+n,N]} = IDFT[UV^*], \quad (4)$$

where n is an integer, the superscript * represents the complex conjugate and $mod\,[a, b]$ is the rest of an integer division of (a:b). A complex value u_n is equal to $u_{mod\,[n,N]}$ when "u" is a periodic sequence with the period N.

When u = v, (4) is defined as the periodic autocorrelation function. A sequence u is called a "perfect sequence" if it has an ideal periodic autocorrelation function proportional to a Dirac unit impulse, $\delta[n]$ defined by (5):

$$r_{uu}[n] = N\delta[n] = \begin{cases} N, & mod\,[n, N] = 0 \\ 0, & mod\,[n, N] \neq 0 \end{cases}. \quad (5)$$

As it is known ($\delta[n] = IDFT[1]$), any sequence of constant amplitude in the frequency domain corresponds to a perfect sequence in the time domain.

The IDFT of a constant sequence (such as a sequence of ones) results in a Dirac unit impulse (also known as the Kronecker delta function) in the discrete-time domain.

Here is the detailed reasoning:

Given a sequence $|U_k|$=1 for k=0,1,…,N−1, which means $|U_k|$ is constant and equal to 1 for all k, the IDFT[$|U_k|$] of (4) is computed. The terms W_N^{-kn} are evenly distributed around the unit circle in the complex plane, and their sum is zero due to symmetry.

Thus, the sequence $u_n = IDFT[U_k]$ is as follows (6):

$$r_{u_n} = \begin{cases} 1, & if \quad mod\,[n, N] = 0 \\ 0, & if \quad mod\,[n, N] \neq 0 \end{cases}. \quad (6)$$

Considering one period, this is the discrete-time equivalent of the Dirac unit impulse, often represented as $\delta[n]$ on equation (7):

$$r_{u_n} = \delta[n]. \quad (7)$$

Therefore, the IDFT of a constant sequence $|U_k| = 1$ is indeed a Dirac unit impulse.

In other words, we can say that the sequence (8):

$$u_{perfect}[n] = \sqrt{N} \times IDFT[U_k], \quad (8)$$

when $0 \leq n, k \leq N - 1$, is a normalized perfect sequence if

$$|U_k|^2 = 1. \quad (9)$$

Using (8) we can generate perfect sequences (with constant envelope or not) of any length N, when it $|u_n|$ is constant for all values $0 \leq n \leq N - 1$. However, what is usually intended with communication systems is to find perfect sequences with good correlation properties. For example, perfect sequences with low cross-correlation values (in absolute value).

Ideally, sequences used in Code Division Multiple Access (CDMA-type) systems or Orthogonal Frequency-Divi-

sion Multiplexing - Code Division Multiple Access (ODFM-type) systems should have a perfect periodic autocorrelation function [12-14] when multi-path interference is predominant. In other words, the perfect periodic autocorrelation function must be equal to the function of a Dirac unit impulse $\delta[n]$. However, since bipolar sequences with the perfect periodic autocorrelation function are not known except for x = {1, 1, 1, -1} or for any cyclic rotation of x [15, 16], it is desirable to find new sequences. Alternative solutions can be found with periodic complex sequences defined by some authors as sequences of multiple small or large alphabet phases [12, 17, 18], unimodular perfect sequences [19], codes of the type "Phase Shift Pulse" [20], perfect sequences of the root of the unit [21], sequences of Bent functions [22], or simply as perfect sequences [23-25]. Additionally, perfect sequences with four phases (small alphabet) exist for lengths N equal to 2, 4, 8, 16 (Milewski sequences and Frank sequences). Many other sequences with perfect periodic autocorrelation function can be found if a mathematical transformation is used [13,14].

Codes with a near-perfect periodic autocorrelation function and that have a reduced MaxCC (maximum periodic cross-correlation in absolute value) can be applied in asynchronous CDMA communication systems, for fast equalization, for estimation of a communication channel, for synchronization, or in other applications impaired by strong interference of the multiple paths type [26].

As already mentioned, a variety of perfect sequences have been proposed by several authors/researchers. The lower bound of the maximum absolute cross-correlation value MaxCC is a constant equal to $\sqrt{N}$ [2, 11, 27]. It is interesting to note that, theoretically, it should not be possible to generate perfect sequences with zero periodic cross-correlation for any temporal displacement.

3. OPDG code generator

Figure 1 depicts a simplified diagram of the application of real OPDG codes in a data communication system in the presence of noise [8]. It illustrates the integration of electronic circuits for coding and decoding OPDG sequences within the communication system.

- The OPDG encoder (block 101) represents the circuits in **Figures 2**(**a**) and **2**(**b**).
- The circuit transforming the sequences is shown as the 'floor of the encoder with DAC' (block 102), representing **Figures 3**(**a**) and **3**(**b**).
- The 'Transmission medium' (block 103) indicates the means of transmission, receiving the sequences with additive noise.
- The 'floor of the decoder with ADC' (block 104) includes an ADC converter and filters to minimize noise effects.
- The OPDG decoder (block 105) corresponds to the circuits in **Figures 4**(**a**), **4**(**b**), or the simplified circuit in **Figure 6**.

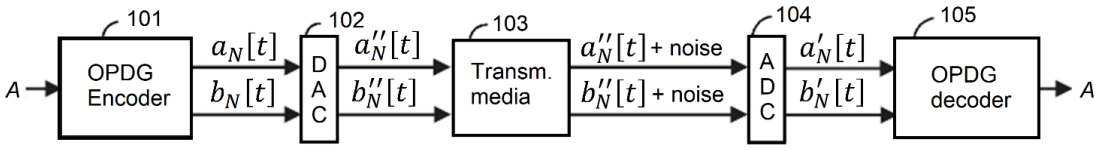

Figure 1. Block diagram of the proposed solution.

The OPDG coding block (101) serves as the electronic generator of OPDG codes, while the OPDG decoder (105) acts as the electronic detector of OPDG codes transmitted in a CDMA medium (103) with noise or electronic interference. The information transmitted by the user is proportional to the detection of the assigned OPDG code.

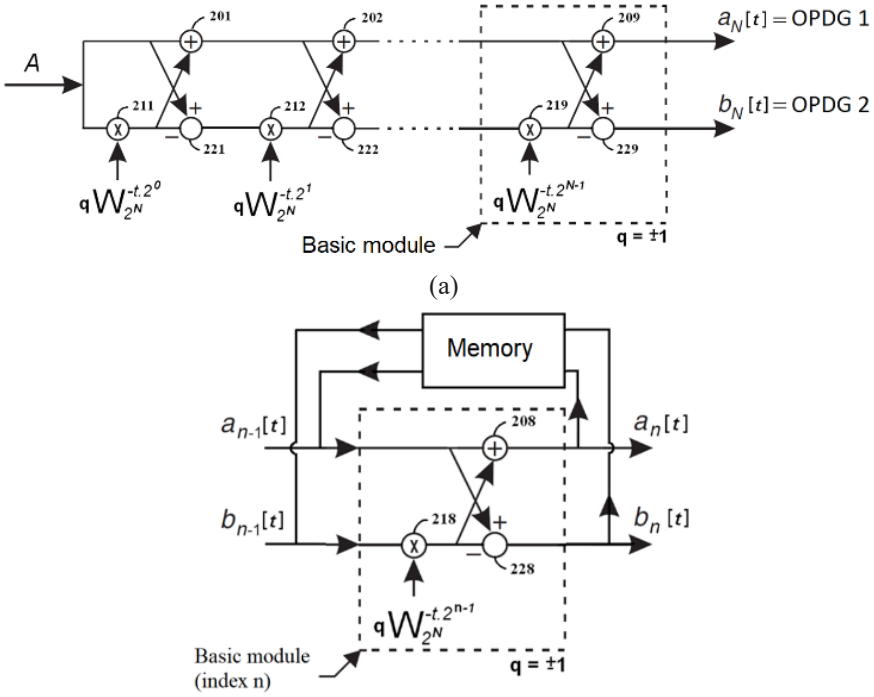

Figure 2. (**a**) Hardware implementation of the generator circuit (encoder) of a pair of perfect orthogonal sequences (**b**) Hardware implementation of the electronic encoder of OPDG codes using recursive process.

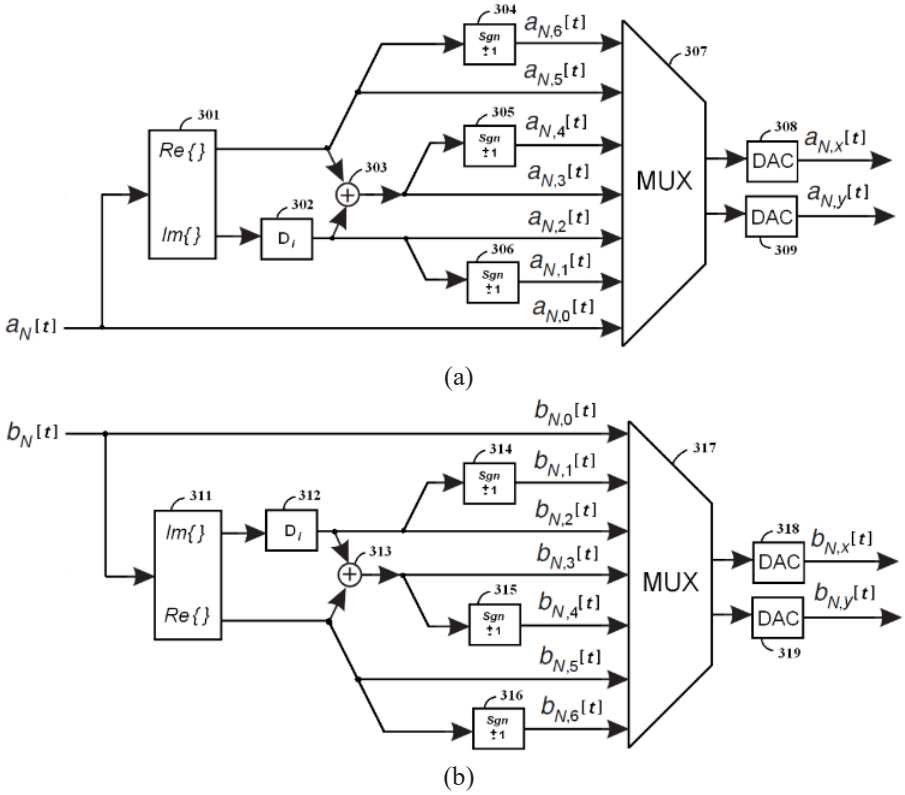

Figure 3. (**a**) Transformation of the complex sequence a_N shows how to apply a set of electronic transformations

to codes. (**b**) Transformation of the complex sequence b_N illustrates how to apply the same set of electronic transformations to codes.

Figure 2(**a**) illustrates the generator circuit (encoder) of a pair of perfect orthogonal sequences. The perfect sequences aN[t] is called the OPDG code 1 and bN[t] is called the OPDG code 2.

- The generator circuit produces a pair of discrete orthogonal and perfect sequences, OPDG 1 and OPDG 2, of length L = 2N.
- The encoder incorporates adders, differentiators, and multipliers (multiplying by a vector complex 'twiddle factor' WL = exp (-j2π/L)).
- The value of the 'twiddle factor' in each module is crucial for generating OPDG codes with perfect autocorrelation and zero cross-correlation.

Figure 2(**b**) shows the hardware implementation of the coder of OPDG codes using a recursive process.

- This method employs a single module called recursively N times, advantageous when N is high.
- The recursive process involves input vectors an-1[t] and bn-1[t] and output vectors an[t] and bn[t], with n as an integer (1 ≤ n ≤ N).
- The initial condition is $a_0[t] = A$ and $b_0[t] = A$, where A is a real constant vector or signal, performed only at the first iteration (n = 1).

Mathematical Proofs

Golay Sequences Recap

We start with the Golay sequences generated using Budisin's recursive method [28], defined as (10-13):

$$A_0[k] = \delta[k] \quad (10)$$

$$B_0[k] = \delta[k] \quad (11)$$

$$A_n[k] = A_{n-1}[k] + q.B_{n-1}[k - D_n] \quad (12)$$

$$B_n[k] = A_{n-1}[k] - q.B_{n-1}[k - D_n]. \quad (13)$$

After applying the IDFT to the bipolar Golay sequences (12) and (13), we get the sequences $a_n[t]$ and $b_n[t]$ as follows (14,15):

$$a_n[t] = a_{n-1}[t] + q.W_{2^N}^{-t.2^{n-1}}.b_{n-1}[t] \quad (14)$$

$$b_n[t] = a_{n-1}[t] - q.W_{2^N}^{-t.2^{n-1}}.b_{n-1}[t]. \quad (15)$$

Here, $q = \pm 1$.

The initial condition is $a_0[t] = A$ and $b_0[t] = A$, where A is a real constant vector or signal, and each electronic module uses a complex hardware implementation equal to (16):

$$q.W_{2^N}^{-t.2^{n-1}}. \quad (16)$$

Length L = 2N, with WL = exp(-j2π/L).

Autocorrelation Analysis

Autocorrelation of $a_n[t]$

The autocorrelation function of $a_n[t]$ is defined as (17,18):

$$R_{a_n a_n}[m] = \sum_{t=0}^{L-1} a_n[t] \cdot a_n[t+m] \quad (17)$$

$$a_n[t] = a_{n-1}[t] + q \cdot W_{2N}^{-t.2^{n-1}} \cdot b_{n-1}[t] \quad (18)$$

The autocorrelation becomes (19):

$$R_{a_n a_n}[m] = \sum_{t=0}^{L-1} \left(a_{n-1}[t] + q \cdot W_{2N}^{-t.2^{n-1}} \cdot b_{n-1}[t]\right)\left(a_{n-1}[t+m] + q \cdot W_{2N}^{-(t+m).2^{n-1}} \cdot b_{n-1}[t+m]\right) \quad (19)$$

Expansion of Terms

Breaking it down, we have (20):

$$R_{a_n a_n}[m] = \sum_{t=0}^{L-1} \left[a_{n-1}[t] a_{n-1}[t+m] + q \cdot W_{2N}^{-(t+m)\cdot 2^{n-1}} a_{n-1}[t] b_{n-1}[t+m] \right]$$

$$\left(+q \cdot W_{2N}^{-t\cdot 2^{n-1}} b_{n-1}[t] a_{n-1}[t+m] + |q|^2 \cdot b_{n-1}[t] b_{n-1}[t+m] \right) \quad (20)$$

Simplification Using Complementary Properties

First and Last Terms: The terms $a_{n-1}[t]a_{n-1}[t+m]$ and $b_{n-1}[t]b_{n-1}[t+m]$ contribute significantly at zero offset due to the Golay sequence's autocorrelation property, maintaining the main peak.

Mixed Terms Cancellation: The mixed terms $q \cdot W_{2N}^{-(t+m)\cdot 2^{n-1}} a_{n-1}[t] b_{n-1}[t+m]$ and $q \cdot W_{2N}^{-t\cdot 2^{n-1}} b_{n-1}[t] a_{n-1}[t+m]$ cancel for $m \neq 0$, thanks to the orthogonal properties imposed by the phase shifts W_{2N}.

Result: This ensures $R_{a_n a_n}[m] \approx \delta[m]$, resulting in a Dirac-like impulse for the autocorrelation.

Cross-Correlation Analysis

Cross-Correlation between $a_n[t]$ and $b_n[t]$

The cross-correlation function is (21):

$$R_{a_n b_n}[m] = \sum_{t=0}^{L-1} a_n[t] \cdot b_n[t+m] \quad (21)$$

Using the recursive definitions we have (22, 23):

$$a_n[t] = a_{n-1}[t] + q \cdot W_{2N}^{-t\cdot 2^{n-1}} \cdot b_{n-1}[t] \quad (22)$$

$$b_n[t] = a_{n-1}[t] - q \cdot W_{2N}^{-t\cdot 2^{n-1}} \cdot b_{n-1}[t] \quad (23)$$

Substitute to get (24, 25):

$$R_{a_n b_n}[m] = \sum_{t=0}^{L-1} \left(a_{n-1}[t] + q \cdot W_{2N}^{-t\cdot 2^{n-1}} b_{n-1}[t] \right) \left(a_{n-1}[t+m] - q \cdot W_{2N}^{-(t+m)\cdot 2^{n-1}} b_{n-1}[t+m] \right) \quad (24)$$

$$R_{a_n b_n}[m] = \sum_{t=0}^{L-1} \left[a_{n-1}[t] a_{n-1}[t+m] - q \cdot W_{2N}^{-(t+m)\cdot 2^{n-1}} a_{n-1}[t] b_{n-1}[t+m] \right]$$

$$\left(+q \cdot W_{2N}^{-t\cdot 2^{n-1}} b_{n-1}[t] a_{n-1}[t+m] - |q|^2 \cdot b_{n-1}[t] b_{n-1}[t+m] \right) \quad (25)$$

Simplification

Mixed Terms Cancellation: The terms $q \cdot W_{2N}^{-(t+m)\cdot 2^{n-1}} a_{n-1}[t] b_{n-1}[t+m]$ and $q \cdot W_{2N}^{-t\cdot 2^{n-1}} b_{n-1}[t] a_{n-1}[t+m]$ cancel each other, significantly reducing cross-correlation contributions.

Zero Cross-Correlation: The structure ensures that $R_{a_n b_n}[m] \approx 0$, ensuring near-zero cross-correlation.

Mathematical Proof of the Orthogonality of $\mathrm{Re}(a_n[t])$ and $\mathrm{Im}(a_n[t])$ for Any Cyclic Translation t

Let's prove the orthogonality of the real and imaginary parts of the sequences $a_n[t]$ and $b_n[t]$ generated by applying the IDFT to Golay pairs. We aim to show that for any cyclic translation t (26):

$$\sum_{t=0}^{L-1} \mathrm{Re}\,(a_n[t]) \cdot \mathrm{Im}(a_n[t+m]) = 0 \quad (26)$$

for any m, where $L = 2^N$ is the sequence length.

Step-by-Step Proof

Expand $a_n[t]$ in terms of real and imaginary parts (27):

$$a_n[t] = \mathrm{Re}(a_n[t]) + j \cdot \mathrm{Im}(a_n[t]) \quad (27)$$

and similarly for $b_n[t]$.

Substitute the recursive definition:

$$a_n[t] = \mathrm{Re}\left(a_{n-1}[t] + q \cdot W_{2^N}^{-t\cdot 2^{n-1}} \cdot b_{n-1}[t] \right) + j \cdot \mathrm{Im}\left(a_{n-1}[t] + q \cdot W_{2^N}^{-t\cdot 2^{n-1}} \cdot b_{n-1}[t] \right)$$

Orthogonality condition: The condition for orthogonality between $\mathrm{Re}(a_n[t])$ and $\mathrm{Im}(a_n[t+m])$ requires that (28):

$$\sum_{t=0}^{L-1} \mathrm{Re}\,(a_n[t]) \cdot \mathrm{Im}(a_n[t+m]) = 0 \quad (28)$$

for all m.

This means the real and imaginary parts are uncorrelated for any shift $\boldsymbol{m}$.

Recursive nature and symmetry: The recursive nature of $\boldsymbol{a_n[t]}$ and $\boldsymbol{b_n[t]}$ ensures that both the real and imaginary parts are constructed in such a way that they are balanced (i.e., their contributions cancel out over a full cycle of length $\boldsymbol{L}$). Given the symmetry and the orthogonality properties imposed by the IDFT and Golay sequences, we get (29):

$$\sum_{t=0}^{L-1} \mathrm{Re}\,(a_n[t]) \cdot \mathrm{Im}(a_n[t+m]) = \mathrm{Re}\big(DFT\big[a_n[t]\big]\big) \cdot \mathrm{Im}\big(DFT\big[b_n[t]\big]\big) + \mathrm{Re}\big(DFT\big[b_n[t]\big]\big) \cdot \mathrm{Im}\big(DFT\big[a_n[t]\big]\big) = 0 \quad (29)$$

due to the orthogonality and symmetry in the frequency domain.

General result: The same logic applies to $\boldsymbol{b_n[t]}$, proving that the real and imaginary parts of the sequences $\boldsymbol{a_n[t]}$ and $\boldsymbol{b_n[t]}$ are orthogonal under any cyclic translation.

Why this property is rare and useful in communication systems?

Rarity: Orthogonality between the real and imaginary parts of sequences after cyclic shifts is rare because it requires a careful balance in the construction of the sequences. Most random sequences do not exhibit this property due to the lack of inherent structure and symmetry.

Utility in communication systems:

Improved Signal Separation: Orthogonality between the real and imaginary parts means that these components can be separated cleanly, which is particularly useful in quadrature amplitude modulation (QAM) schemes where signals are transmitted using both real and imaginary components.

Reduced Interference: In systems where multiple sequences are used simultaneously (e.g., CDMA), orthogonal components reduce the likelihood of cross-interference, leading to cleaner signal detection and decoding.

Enhanced Multiplexing: With orthogonal real and imaginary parts, it becomes easier to multiplex different data streams in a way that minimizes interference, enhancing the overall system capacity.

In summary, the orthogonality of $\mathrm{Re}(\boldsymbol{a_n[t]})$ and $\mathrm{Im}(\boldsymbol{a_n[t]})$ (and similarly for $\mathrm{Re}(\boldsymbol{b_n[t]})$ and $\mathrm{Im}(\boldsymbol{b_n[t]})$) is a direct consequence of the structured recursive construction of the sequences and the inherent symmetry and balance provided by the IDFT of Golay pairs. This property is highly desirable in communication systems due to its ability to reduce interference and enhance signal clarity, especially in complex modulation schemes.

In **Fig. 2** (**b**) the two outputs (14) and (15) are stored in a memory component before being injected into the two inputs of the basic electronic module (with index n) in the next iteration. The hardware implementation of the encoder of OPDG codes alternative to that of **Figure 2**(**a**) incorporates an adder, a differentiator and a multiplier.

Figure 3(**a**) is a complex sequence a_N transformation, and shows how to apply a set of hardware implementations to codes $a_N[t]$; and **Figure 3**(**b**) shows transformation of the complex sequence b_N, and illustrates how to apply the same set of hardware implementations to the codes $b_N[t]$. **Figures 3**(**a**) and **3**(**b**) are complementary to **Figure 2**(**a**). The OPDG codes 1, in **Figure 2**(**a**), will be the entry codes in **Figure 3**(**a**). The OPDG 2 codes, in **Figure 2**(a), will be the entry codes in **Figure 3**(**b**). The multiplexers (307) and (317) will allow the user to use the desired exit codes which can be $a_{N,X}[t]$, $a_{N,Y}[t]$, $b_{N,X}[t]$ and $b_{N,Y}[t]$.

The hardware implementation of the encoder in **Figure 2**(**a**), of an OPDG code pair, requires an hardware implementation of the decoder capable of reversing the operation of the specific encoding.

Figure 4(**a**) represents the decoder circuit of a pair of perfect orthogonal sequences $a_N[t]$ and $b_N[t]$, consisting of N basic electronic modules. Each basic electronic module consists of an adder, a differentiator and a multiplier by a complex hardware implementation derived from a "twiddle factor" (WL = exp (j2π/L)) specific to each electronic modules. The specific connections of the three operators, of the basic module of **Figure 4**(**a**), allow the electronic decoding of OPDG codes of a certain length. This hardware implementation is a recursive process, that is, the decoding of an OPDG code of length 2N is obtained based on the electronic decoding of a code of length 2N-1. The entry codes $a_N^{'}[t]$

and $b_N^{'}[t]$, the first basic module of **Figure 4**(**a**), can be the same as the codes $a_N[t]$ and $b_N[t]$ of **Figure 2**(**a**), respectively. However, entry codes $a_N^{'}[t]$ and $b_N^{'}[t]$ may also be the codes $a_{N,X}[t]$, $a_{N,Y}[t]$, $b_{N,X}[t]$ and $b_{N,Y}[t]$, of **Figures 3**(**a**) and (**b**). In addition, entry codes $a_N^{'}[t]$ and $b_N[t]$ may also be the codes referred to above when they are contaminated by noise or another source of electronic interference. The block (432) of **Figure 4**(**a**) performs the electronic operation 'real part' of an FFT (Fast Fourier Transform) that allows generating the signal equal to a Dirac unit impulse with amplitude A[q]N22N+1. This impulse will appear to be temporarily displaced by a 2N-1 value.

Figure 4(**b**) shows the electronic OPDG code decoder (105) when the basic modules are used in a recursive process. Instead of having N electronic modules connected in a chain, only one is used which is called recursively N times. This method is advantageous when the N value is high. The recursive process is defined by two complex input vectors $a_n[t]$ and $b_n[t]$, and two complex output vectors $a_{n-1}[t]$ and $b_{n-1}[t]$, where n is an integer. The output is the same as the expression (30):

$$a_{n-1}[t] = q.W_{2^N}^{-t2^{n-1}}.\{a_n[t] + b_n[t]\}. \tag{30}$$

The output $b_{n-1}[t]$ is equal to the expression (31)

$$b_{n-1}[t] = a_n[t] - b_n[t], \tag{31}$$

with $q = \pm 1$.

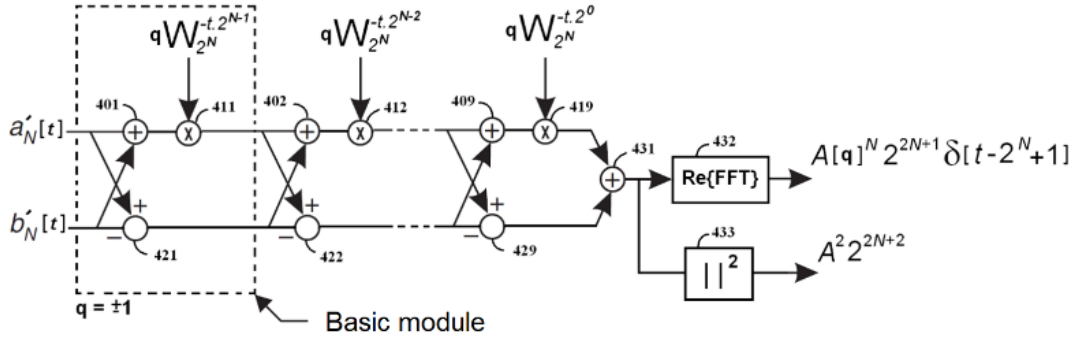

(a)

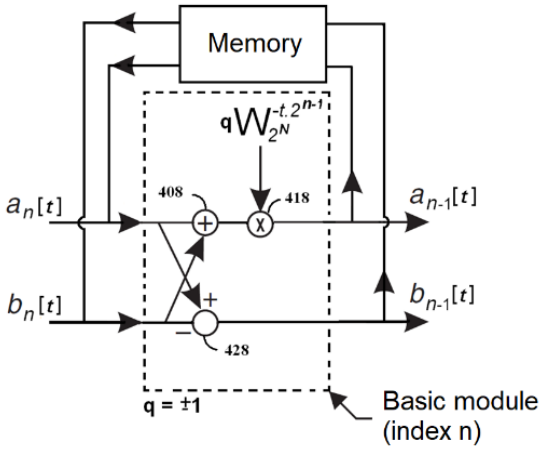

(b)

Figure 4. (**a**) Decoder circuit of a pair of perfect orthogonal sequences (**b**) OPDG hardware implementation of the decoder (105) when the basic modules are used in a recursive process.

In the last iteration, two output vectors $a_0[t]$ and $b_0[t]$ are added together to generate a unimodular complex vector. Each specific module of an iteration, represented by an index n, uses a complex vector equal to (32)

$$q.W_{2^N}^{-t.2^{n-1}} \tag{32}$$

of length L = 2N, where WL = exp(-j2π/L).

The two outputs $a_{n-1}[t]$ and $b_{n-1}[t]$ of the electronic module are stored in a memory component before being injected into the two inputs of the basic electronic module (index n) in the next iteration. The initial condition is and is only performed the first time, at the first iteration n = N. Unlike the OPDG encoder, here the iteration index is decremented by one, starting at n = N and ending at n = 1.

Figure 5 depicts a simplified diagram of the application of bipolar codes OPDG {-1, +1} in a data communication system in the presence of noise, illustrating the communication system of **Figure 1** when a single signal $a_{N,4}[t]$, of **Figure 3**(**a**), is used and transmitted by the transmission medium (603). This signal is a bipolar sequence {-1, +1} that depends on the cyclical displacement Di (302) applied. Because the value i can take L different values ($0 \leq i < L$), it will be possible to generate L different bipolar sequences of length L. These bipolar codes have excellent correlation properties. The detection of the correct sequence can be done with an electronic circuit that allows estimating the value of the autocorrelation.

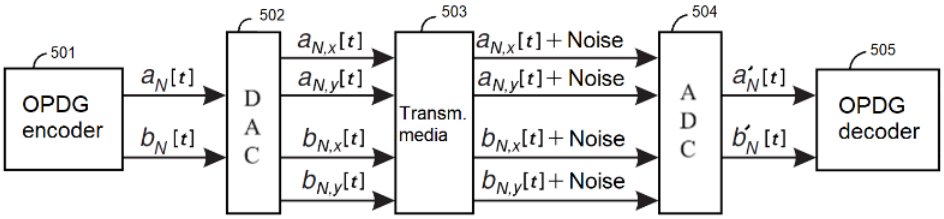

Figure 5. Simplified illustration of the application of bipolar codes OPDG in a data communication system with noise.

Figure 6 depicts a circuit that implements a classic correlation function where the input signal is multiplied by the sequence $a'_{N,4}[t]$ (which has a specific cyclic shift i). The integrator will electronically implement a sum of L discrete elements. This circuit is an alternative to the decoder of **Figures 4**(**a**) and **4**(**b**), when the strings have a short length. When the length (L = 2N) is long, it is preferable to use the circuit of the **Figures 4**(**a**) or **4**(**b**).

Figure 7 shows a correlation function between the vector received $a'_{N,4}[t]$ and the reference vector $a'_{N,4}[t]$. The multiplication of this correlation function is performed by the block (701) and the integration (or summation) function is performed by the block (702).

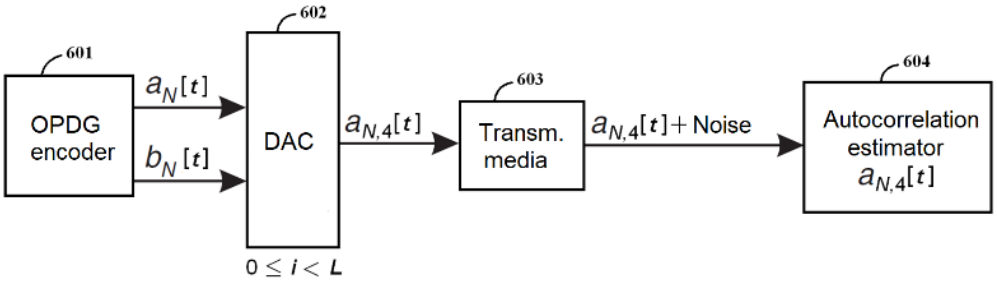

Figure 6. Simplified application of bipolar codes OPDG {-1, +1} in a data communication system in the presence of noise.

Figure 8 illustrates the implementation of the electronic circuit encoding in **Figure 2**(**a**) when N = 5. Five basic electronic modules in **Figure 2** were used. Figure 8 is equivalent to the generator of **Figure 2**(**a**) when there are 5 basic electronic modules that allow the generation of OPDG codes of length 32.

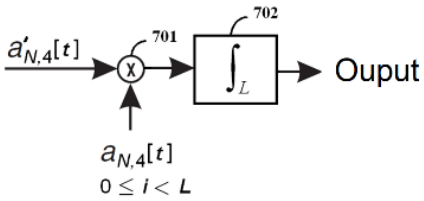

Figure 7. Circuit to perform a correlation function of the codes $a'_{N,4}[t]$.

When N = 5, the normalized periodic autocorrelation function of OPDG1 (and OPDG2) is qual to $\delta[n]$ and the periodic cross-correlation between OPDG1 and OPDG2 has a maximum value equal to 1/16. This maximum value is lower than the maximum value of the normalized periodic cross-correlation between the two Golay sequences of the same length 32.

Figure 9 illustrates the hardware implementation of the decoder circuit of **Figure 4**(**a**) when N = 5. Five basic electronic modules of **Figure 4**(**a**) were used. Depending on the type of application, blocks (932) and (933) may be omitted. **Figure 9** represents the hardware implementation of the decoder of the OPDG codes of **Figure 2**(**a**) when the hardware implementation of the encoder consists of 5 basic electronic modules.

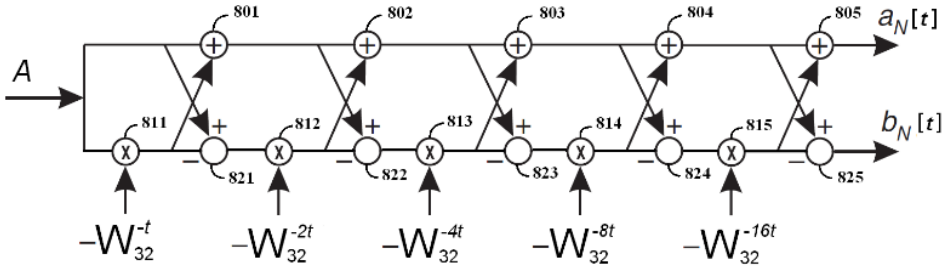

Figure 8. Generator circuit (encoder) of a pair of OPDG sequences of length 32.

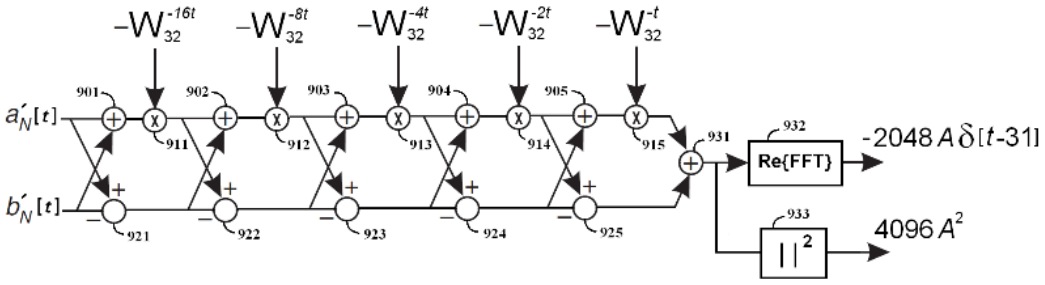

Figure 9. Decoder circuit of a pair of OPDG sequences of length 32.

Figure 10 represents some periodic autocorrelation functions for different codes generated based on the encoder in **Figure 8**. The superiority of the OPDG 1 and OPDG 2 codes are highlighted in relation to the Golay codes. The periodic autocorrelations of the OPDG 1, OPDG 2, [Re (OPDG 1) + Im (OPDG 1)] and [Re (OPDG 2) + Im (OPDG 2)] sequences are proportional to a Dirac unit impulse. This does not happen with the complementary Golay code pairs (Golay 1 and Golay 2).

Figure 11 represents the periodic cross correlation functions for different codes. The complementary sequences Re(OPDG 1) and Im(OPDG 1) are orthogonal to any cyclic shifts with $0 \leq i < L$. The same happens with the pair of sequences Re(OPDG 2) and Im(OPDG 2), but not with the complementary pairs of Golay (Golay 1 and Golay 2). In this last property lies the great difference between the Golay codes and the OPDG codes of the present codec.

Figure 12 represents aperiodic cross correlation functions for different codes. A pair of complementary sequences Re(OPDG 1) and Im(OPDG 1) has low correlation values for any cyclic shifts with $0 \leq i < L$. The same happens with the pair of sequences Re(OPDG 2) and Im(OPDG 2), but it is not so efficient with the complementary pairs of Golay (Golay 1 and Golay 2).

Figure 13 presents absolute values of the aperiodic autocorrelation functions for bipolar codes. The bipolar sequences derived from the OPDG sequences have maximum, lagged, absolute values lower than those of the Golay sequences.

Finally, **Figure 14** shows the absolute values of the periodic autocorrelation functions for four bipolar codes, with better values than Golay sequences.

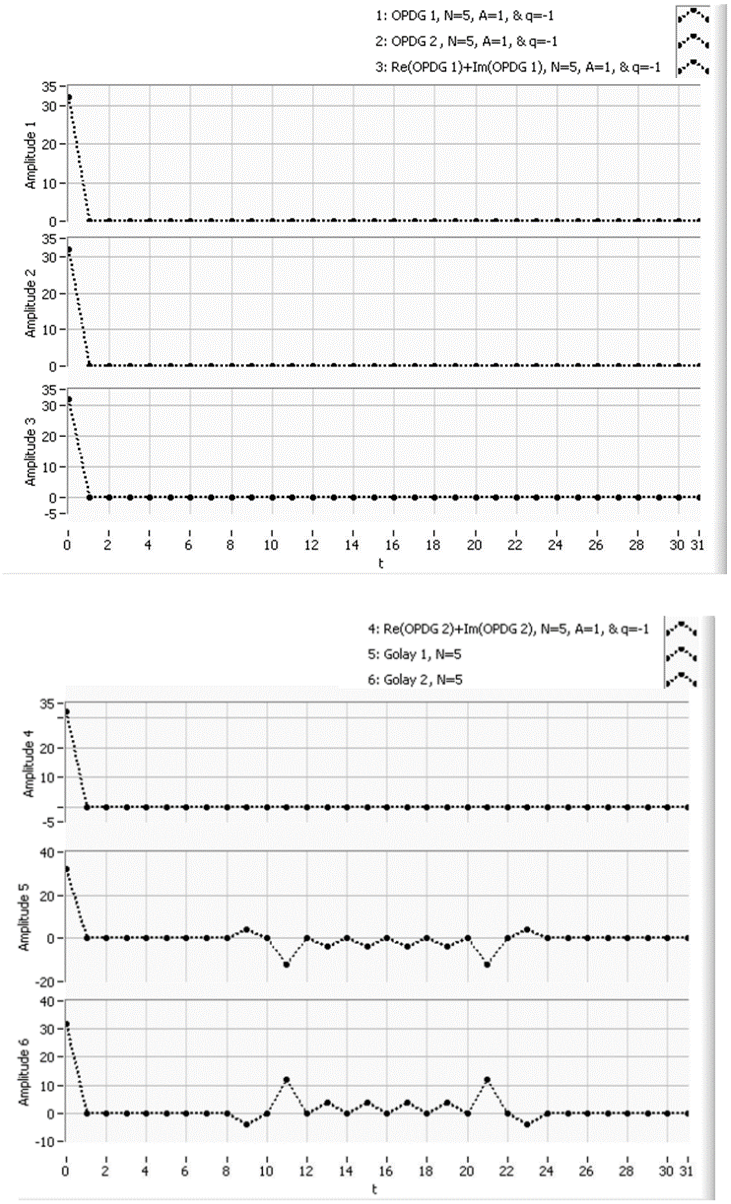

Figure 10. Periodic autocorrelation functions for various codes.

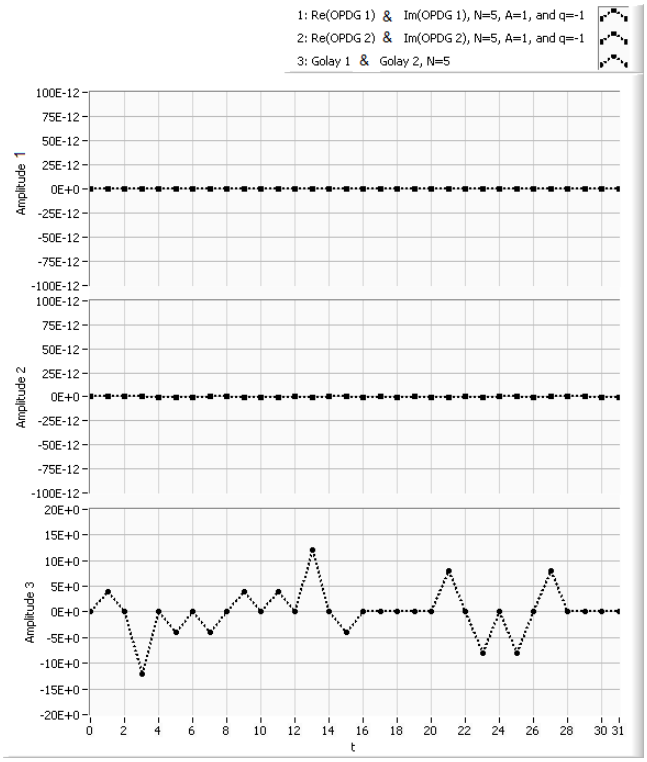

Figure 11. Periodic cross correlation functions for different codes showing complementary sequences having low correlation values for any cyclic shifts.

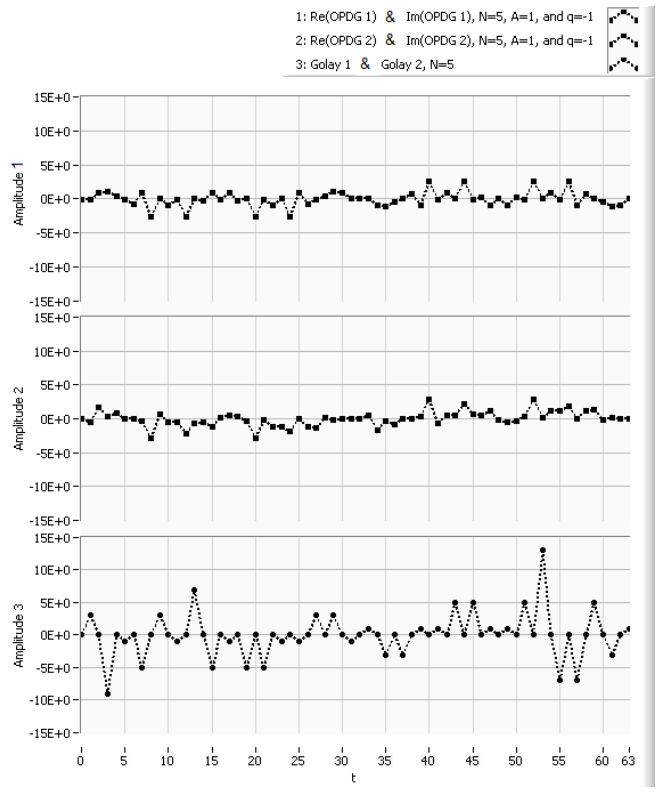

Figure 12. Absolute values of the aperiodic cross correlation functions for bipolar codes.

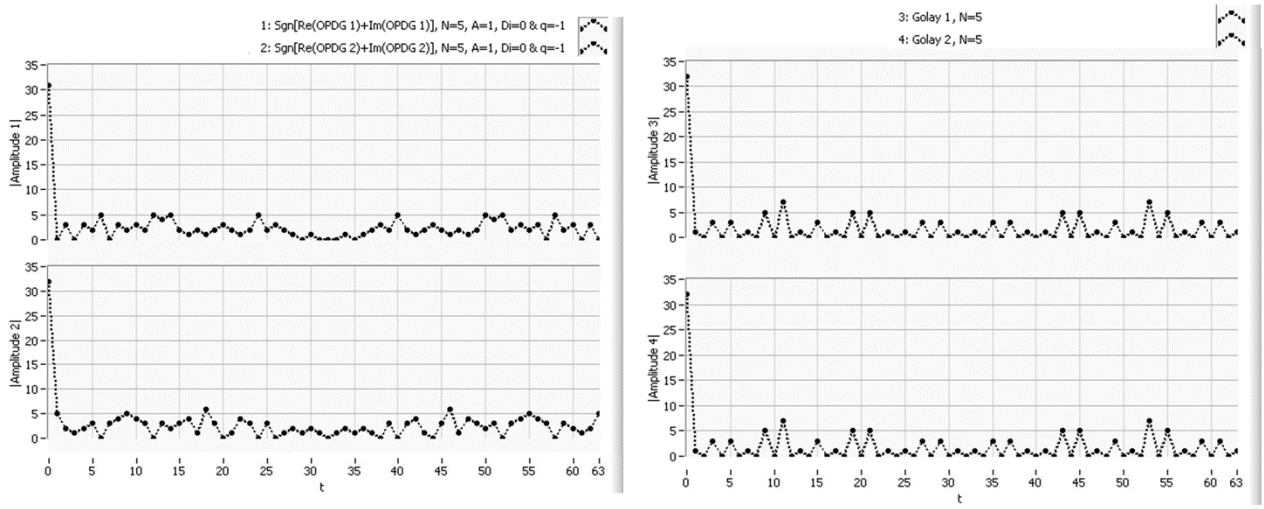

Figure 13. Absolute values of the aperiodic autocorrelation functions for four bipolar codes.

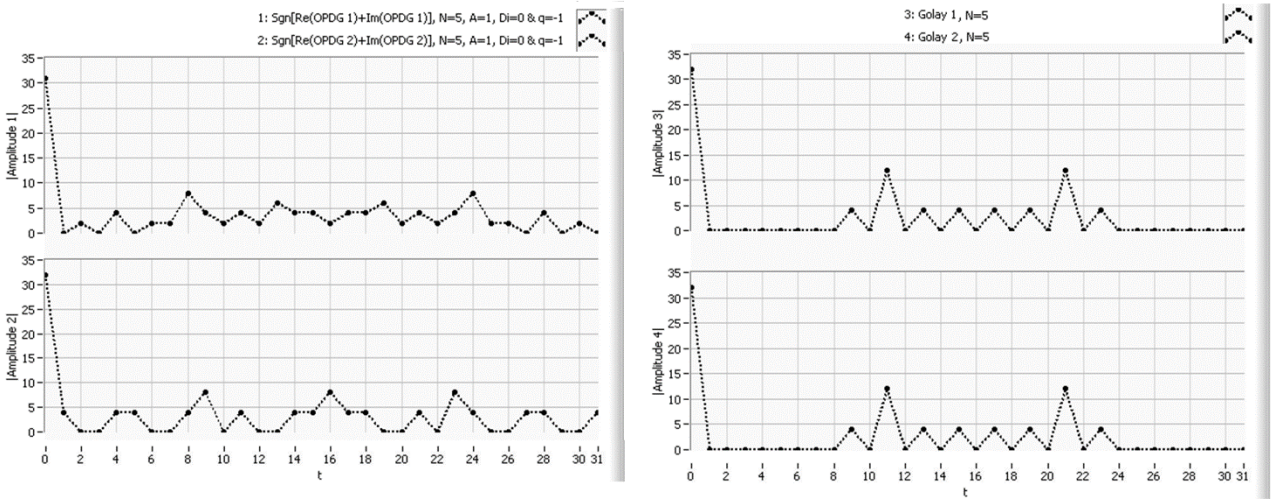

Figure 14. Absolute values of the periodic autocorrelation functions for four bipolar codes.

4. Error probability

To streamline the study and analysis of the PAPR solution through binary decomposition, we opted to focus exclusively on bipolar codes. In this context, a straightforward CDMA system is suitable for evaluating these new bipolar codes. The phase modulation utilized is a simple Binary Phase-Shift Keying (BPSK) modulation, allowing us to employ a known error probability P_e to establish an upper bound for the CDMA system. This upper bound, $max\{P_e\}$, can be expressed as a function of the cross-correlation power contrast ratio, $P/C = 20\ log\left[r_k(0)/max\{r_{k,i}\}\right]$ (in dB), where $r_{k,i}$ represents the cross-correlation and r_k denotes the autocorrelation [27].

Several upper bounds for P/C, applicable to periodic correlations, have been identified. One notable example is the Welch bound [25] for K perfect sequences of length N, given by (33):

$$P/C = 20\,log\sqrt{(KN-1)/(K-1)}. \tag{33}$$

For the case of aperiodic correlation, the upper bound is (34):

$$P/C = 20\log\sqrt{(2KN - K - 1)/(K - 1)}. \quad (34)$$

For an effective communication system, any set of codes should exhibit a high power contrast ratio. For instance, it has been recommended that codes should have power contrast ratios exceeding 17 dB for 127-chip Gold codes [28]. In this study, we examine the upper bound of the error probability, which is a function of the power contrast ratio P/C (35):

$$max\{P_e\} = 1 - \emptyset\left[\left(\frac{N_0}{2E_b} + (K-1)(1-\frac{1}{L})10^{-\frac{P/C}{10}}\right)^{-1/2}\right]. \quad (35)$$

Figures 15 and **16** illustrate the variation in error probabilities as a function of the number of simultaneously used codes. These graphs demonstrate the superiority of bipolar codes derived from OPDG sequences over Gold codes of equivalent length and quantity. The favorable autocorrelation and cross-correlation properties of these codes make them particularly well-suited for use in CDMA communication systems.

The proposed method enables the generation of optimal code sets in quantities equal to the length L. Additionally, due to their low cross-correlation values, a receiver can effectively extract its designated code and binary information even when all other codes are transmitted simultaneously. In essence, the codes generated by the new CODEC are highly resistant to interference, both from multipath effects and from adjacent communication channels.

Figures 15 and **16** reveal that bipolar codes derived from OPDG codes presents lower error probability than the well-known orthogonal Gold codes, when 4 codes are transmitted simultaneously in a CDMA systems with BPSK modulation.

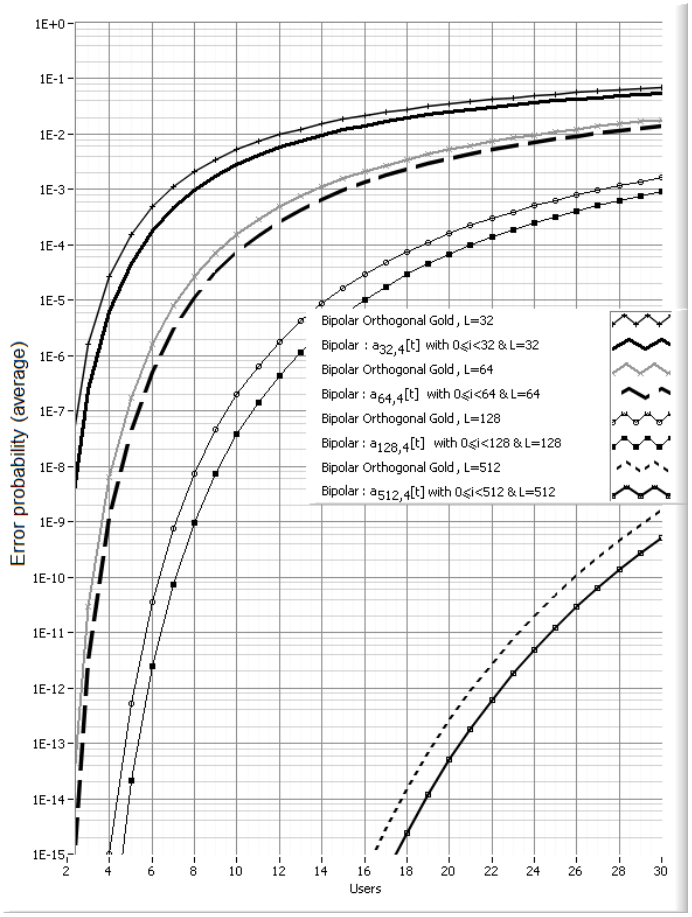

Figure 15. Probability of error according to the number of codes used simultaneously.

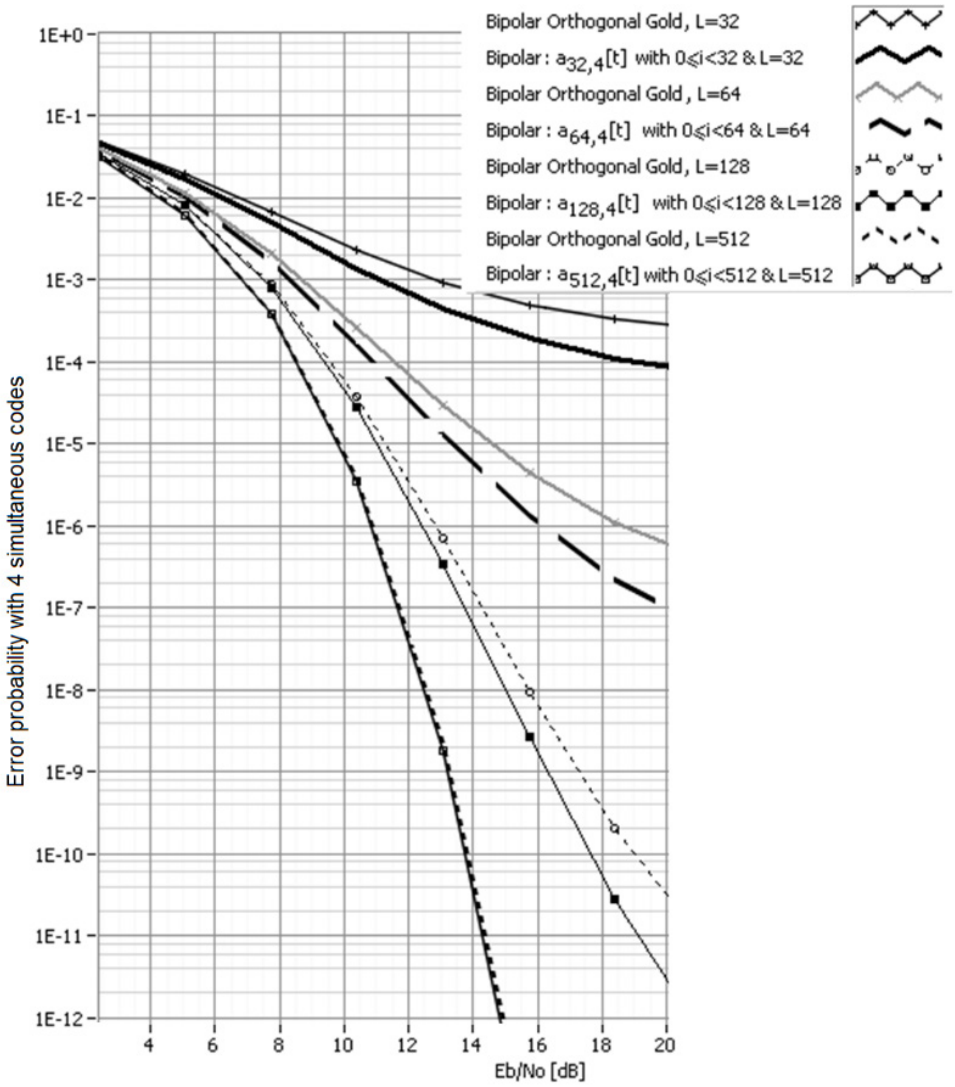

Figure 16. Probability of error as a function of Eb/No.

5. PAPR Solution with Binary Decomposition

In an OFDM system, radio frequency signals can exhibit high peak amplitude values in the time domain due to the summation of multiple subcarrier factors via an IDFT operation. Consequently, OFDM systems are known to have a high PAPR compared to single-carrier systems. Decomposed sequences generated by the OPDG generator can be bi-polar {+1, -1} codes, ensuring a minimal PAPR of 1. A real sequence can be decomposed into a sum of several bipolar Seq_n sequences, each having a PAPR of 1 for n = 0, 1,..., N.

The well-known definition of PAPR [29] is given in Equation (36), where $|X_{peak}|$ is the absolute maximum value and Xrms is the root mean square value of the sequence *X*:

$$PAPR = \frac{|X_{peak}|^2}{X_{rms}{}^2} \tag{36}$$

To minimize the PAPR of any *X* sequence, we demonstrate that it is possible to transform *X* into a sum of bipolar

sequences, each with a PAPR of 1. The process begins by converting the complex sequence into two parts (real and imaginary). Each part is then converted into positive sequences by adding a constant offset value if necessary. The sequences are sampled with an Analog-to-Digital Converter (ADC) resolution of N+1 bits and converted into binary numbers within the range [0; 2N+1]. Any positive base-10 number can be expressed as the sum of N+1 weighted base-2 numbers for each sequence element.

In other words, a sequence can be the sum of N+1 Seq_n sequences of any length L, as defined in (37), where n is an integer ranging from 0 to N, and i ranges from 0 to L:

$$Seq_n[i] = Bit\_n[i] \times 2^n - 2^{n-1} \tag{37}$$

Here, Bit_n[i] are the values at each n-level binary conversion, with level zero representing the least significant bit and level N the most significant bit. For example, the transformation of a real sequence is as follows (38):

$$Sgn(X) \cong \frac{Seq\_N[i]}{2^{N-1}}. \tag{38}$$

PAPR is crucial in communication systems because low-cost electronic amplifiers struggle to implement linear functions effectively. However, if the amplifier's response is nonlinear, it can transmit significantly more power at a reduced cost. Rather than using a single amplifier, multiple nonlinear amplifiers can be employed. We propose using N+1 low-cost amplifiers for all Seq_n bipolar sequences (n = 0, 1, ..., N), each with a PAPR of 1. Each Seq_n bipolar sequence can be transmitted separately using N+1 BPSK modulators and low-cost nonlinear amplifiers. Each Seq_n bipolar sequence can be transmitted synchronously in the same channel using N+1 BPSK modulators, effectively utilizing the channel's bandwidth. At the receiver, a MIMO-like (Multiple-input Multiple-output) processing approach can be employed to separate and reconstruct these sequences, leveraging the orthogonality of the sequences or their distinct transmission characteristics. This technique ensures robust signal recovery despite potential channel variations. The proposed method not only minimizes the PAPR across all sequences, allowing for the use of low-cost nonlinear amplifiers, but also improves overall system power efficiency and signal integrity. By capitalizing on MIMO techniques, the system can achieve scalable, high-quality transmission with reduced complexity and cost, making it a practical and efficient solution for modern communication systems.

Figure 17 illustrates the construction of a signal estimator with a resolution of N+1 bits. By decomposing a signal into N+1 bipolar signals and summing these components (at the MIMO-like receiver), we obtain an estimated combined signal $\tilde{X}$. The sum of N+1 Seq_n signals is also depicted in **Figure 17**.

The signal X in Figure 17 can be either a perfect sequence or any other multilevel sequence within the range [-2N; 2N], while the estimated signal $\tilde{X}$ is the sum of the N+1 bipolar sequences (Seq_0, Seq_1, …, Seq_N). Each of these sequences has a PAPR of 1. These N+1 bipolar sequences can be transmitted over separate channels or different BPSK modulation carriers using low-cost nonlinear amplifiers, as shown at the input of amplifier A in **Figure 17**.

Utilizing a single bipolar sequence Seq_N derived from OPDG codes, it is possible to achieve excellent correlation values in CDMA or OFDMA wireless systems employing BPSK modulation. Our comparison between the Seq_N sequences from OPDG codes and Golay codes reveals that OPDG codes significantly outperform Golay sequences in terms of correlation characteristics [8][30]. The performance of CDMA transmission improves with each additional sequence, reducing the error between X and $\tilde{X}$. As anticipated, these bipolar sequences maintain a minimum PAPR [31] value of 1.

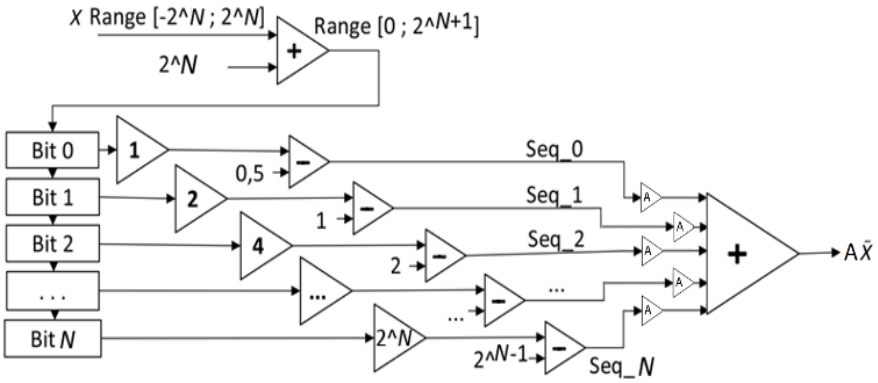

Figure 17. The signal estimation $\tilde{X}$ is the sum of the N bipolar sequences (Seq_0, Seq_1, …, Seq_N).

6. Conclusions

The superiority of bipolar codes derived from OPDG sequences over other orthogonal codes for the same lengths and quantities was demonstrated in this paper. The autocorrelation and cross-correlation of its codes makes it suitable for use in CDMA communication systems. The codes generated by the new CODEC are immune to interference caused by the code itself (multiple paths) and by the other codes.

Using low-cost nonlinear amplifiers to make the amplification of bipolar sequences, before the reconstruction of real sequences, will avoid the PAPR problem. All pre-amplified bipolar sequences will be summed at the end of the reconstruction process (a MIMO-like receiver) to generate the real perfect OPDG sequences with enough power. By this way, the PAPR problem is mitigated and costly linear amplifier are not required.

Author Contributions

Conceptualization, J.P.; methodology, J.P.; software, J.P.; validation, J.P.; formal analysis, J.P.; investigation, J.P.; resources, J.P. and H.F.; data curation, J.P. and H.F.; writing—original draft preparation, J.P. and H.F.; writing—review and editing, J.P. and H.F.; visualization, J.P. and H.F.; supervision, J.P.; project administration, J.P.; funding acquisition, J.P. All authors have read and agreed to the published version of the manuscript.

Funding

This work is funded by Portuguese Fundação para a Ciência e a Tecnologia (FCT/MCTES) through national funds and, when applicable, co-funded by EU funds under the project UIDB/50008/2020.

Institutional Review Board Statement

Not applicable.

Informed Consent Statement

Not applicable.

Data Availability Statement

Not applicable.

Conflicts of Interest

The authors declare no conflict of interest.

References

1. Donato, P. G.; Funes, M. A.; Hadad, M. N.; Carrica, D. O. Optimised golay correlator. Electron. Lett. 2009, 45, 380–381.
2. Fan, P. Z.; Darnell, M.; Honary, B. Crosscorrelations of Frank sequences and Chu sequences. Electron. Lett. 1994, 30, 477–478.
3. Gold, R. Optimal binary sequences for spread spectrum multiplexing. IEEE Trans. Inf. Theory 1967, 13, 619–621.
4. Zhou, Z.; Tang, X.; Peng, D. New optimal quadriphase zero correlation zone sequence sets with mismatched filtering. IEEE Signal Process. Lett. 2009, 16, 636–639.
5. Miller, S. L.; O'dea, R. J. Peak power and bandwidth efficient linear modulation. IEEE Trans. Commun. 1998, 46, 1639–1648.
6. Dardari, D.; Tralli, V.; Vaccari, A. A theoretical characterization of nonlinear distortion effects in OFDM systems. IEEE Trans. Commun. 2000, 48, 1755–1764.
7. Bahl, I. Fundamentals of RF and microwave transistor amplifiers. John Wiley & Sons: Hoboken, NJ, USA, 2009; pp 661 662.
8. Pereira, J. S., & Silva, H. A. Codificador e descodificador eletrónico de sinais ortogonais e perfeitos. Portuguese Patent n.º 106755, 2015,. January 1
9. Theodoridis, S. Machine Learning: A Bayesian and Optimization Perspective, 2nd ed.; Academic Press: Amsterdam, Netherlands, 2020, pp. 1-1160.
10. Oppenheim, A.V.; Schafer, R.W. Digital Signal Processing, 1st ed.; Pearson: Englewood Cliffs, USA, 1975, pp. 1-585.
11. Sarwate, D.V.; Pursley, M.B. Crosscorrelation Properties of Pseudorandom and Related Sequences. In Proceedings of the IEEE Location of Conference, 5 May 1980.
12. Lüke, H.D.; Schotten, H.D.; Hadinejad-Mahram, H. Binary and Quadriphase Sequences With Optimal Autocorrelation Properties: A Survey. IEEE Trans. Inf. Theory 2003, 49, 3271–3282.
13. Fan, P.Z.; Darnell, M. Sequence Design for Communications Applications; Wiley: New York, US, 1996; pp. 1-493.
14. Lüke, H. D. Korrelationsignale. Springer-Verlag: Berlin, Germany, 1992; pp. 1-324.(in German)
15. Schmidt, B. Cyclotomic Integers and Finite Geometry. J. Amer. Math. Soc. 1999, 12, 929–952.
16. Park, S.; Song, I.; Yoon, S.; Lee, J. A New Polyphase Sequence With Perfect Even and Good Odd Cross-Correlation Functions for DS/CDMA Systems. IEEE Trans. Veh. Technol. 2002, 51, 855–866.
17. Popovic, B.M. Generalized Chirp-Like Polyphase Sequences with Optimum Correlation Properties. IEEE Trans. Inf. Theory 1992, 38, 1406–1409.
18. Fan, P.Z.; Darnell, M.; Honary, B. Crosscorrelations of Frank sequences and Chu sequences. Electron. Lett. 1994, 30, 477–478
19. Gabidulin, E. M.; Shorin, V. V. New Families of Unimodular Perfect Sequences of Prime Length Based on Gaussian Periods. In Proceedings of the IEEE International Symposium Information Theory, Lausanne, Switzerland, 30 June 2002.
20. Heimiller, R. C. Phase Shift Pulse Codes with Good Periodic Correlation Properties. IRE Trans. Inf. Theory 1961, 7, 254–257.
21. Mow, W. H. A New Unified Construction of Perfect Root-of-Unity Sequences. In Proceedings of the ISSSTA'95 International Symposium on Spread Spectrum Techniques and Applications, Mainz, Germany, 25 September 1996.
22. Chung, H.; Kumar, P. V. A New General Construction for Generalized Bent Functions. IEEE Trans. Inf. Theory 1989, 35, 206–209.

23. Li, C. P.; Huang, W. C. An Array for Constructing Perfect Sequences and Its Applications in OFDM-CDMA Systems. In Proceedings of the Global Telecommunications Conference, San Francisco, CA, USA, 27 November - 1 December 2006.
24. Li, C. P.; Huang, W. C. A Constructive Representation for the Fourier Dual of the Zadoff–Chu Sequences. IEEE Trans. Inf. Theory 2007, 53, 4221–4224.
25. Fan, P. Z.; Darnell, M. The synthesis of perfect sequences. In Cryptography and Coding; Boyd, C., Eds.; Springe: Berlin, Germany, 1995; 1025, pp. 63–73.
26. Suehiro, N. Pseudo-polyphase orthogonal sequence sets with good cross-correlation property. In Applied Algebra, Algebraic Algorithms and Error-Correcting Codes; Sakata, S., Eds.; Springer: Berlin, Germany, 1991; 508, pp. 106–112.
27. Welch, L. R. Lower Bounds on the Maximum Cross Correlation of Signals. IEEE Trans. Inf. Theory 1974, 20, 397–399.
28. Budisin, S.Z. Efficient pulse compressor for Golay complementary sequences. Electron. Lett. 1991, 27, 219–220.
29. Pereira, J.; Silva, H. A. Orthogonal perfect discrete Fourier transform sequences. IET Signal Process. 2012, 6, 107–113.
30. Pereira, J. Sequências perfeitas para sistemas de comunicação; Novas Edições Acadêmicas: Saarbrücken, Germany, 2015; pp. 1-332. (in Portuguese)
31. Ferreira, M. P. M.; Gasparovic, M.; Manjunath, G.; Mendes, S. P.; Pereira, J. Perfect Periodic Sequences with Low PAPR. In Proceedings of the 2021 Telecoms Conference (ConfTELE), Leiria, Portugal, 11-12 February 2021.